1987A&A...177..204D

Astron. Astrophys. 177, 204–216 (1987)

ASTRONOMY AND ASTROPHYSICS

ζ^1 and ζ^2 Reticuli: a puzzling solar-type twin system *

L. Da Silva [1] **and R. Foy** [2]

[1] Observatorio Nacional, Rua General Bruce, 586, 20921 Rio de Janeiro, Brazil
[2] CERGA, Observatoire du Calern, Caussols, F-06460 Saint-Vallier de Thiey, France

Received March 13, accepted December 5, 1986

Summary. We report the detailed analysis of the solar type stars ζ^1 and ζ^2 Ret. They have solar heavy element abundances and their gravity is found to be abnormally large: $\log g = 4.7$. This, together with their luminosity, typical of subdwarfs, strongly supports the idea that they are significantly helium-rich, with $n(\mathrm{He})/n(\mathrm{H}) = 0.22 \pm 0.04$.

Key words: stellar abundances – helium abundance – solar type stars – moving groups

1. Introduction

We have investigated the twin system $\zeta^1 - \zeta^2$ Reticuli (HD 20766 and HD 20807) in an attempt to understand some apparently conflicting data about these neighbouring stars. They are 310″ apart, with common proper motion and equal radial velocities. As judged from their kinematical parameters, they are likely to be old disc population stars. Woolley (1970) has proposed that they belong to the old moving group ζ Her defined by Eggen (1958). They are classified G2.5 V Fe 1 H 61 (Keenan and Yorka, 1985) or G5V (Koorneff, 1983) for ζ^1 Ret, and G1V (Koorneff, 1983; Keenan and Yorka, 1985) for ζ^2 Ret. Johnson et al. (1968) have included them in a list of subdwarfs, presumably because of their low luminosity. ζ^1 Ret was one of the first stars ever used as a solar analog, namely by Labs and Neckel (1968).

The $U-B$ excesses are $\delta(U-B)_{\zeta^1} = -0.11$ and $\delta(U-B)_{\zeta^2} = -0.14$ (Johnson et al., 1968), or $\delta(U-B)_{\zeta^2} = -0.09$ (Hearnshaw, 1975. $B-V$ and $R-I$ colour indices of ζ^1 Ret do not show significant departures from the mean relationship for main sequence stars (Koornneef, 1983), whereas only the B flux of ζ^2 Ret would be in excess relative to the flux at longer wavelengths. Infrared colour indices lead to cooler effective temperatures than the spectral types do, using the calibrations by Johnson (1966); the colour indices from Koornneef (1983) follow the standard relationship except for U and M. Table 1 summarizes photometric measurements of ζ^1 and ζ^2 Ret.

A UV excess is normally interpreted in terms of a metal deficiency; hence both stars would be markedly metal-poor. But Danziger (1966) found $[\mathrm{Fe/H}]^{\zeta^1}_{\odot} = -0.37$ from a coarse analysis; Foy (1972a) found $[\mathrm{Fe/H}]^{\zeta^1}_{\odot} = -0.1$ from a preliminary detailed analysis; Hearnshaw (1975) derived $[\mathrm{Fe/H}]^{\zeta^2}_{\odot} = -0.32$ from a detailed analysis restricted to Fe I lines. These abundance determinations do not support the interpretation of the UV excess in terms of metallicity.

Conflicting with their belonging to the old disc population is the discovery of emission in the H and K Ca II lines (Foy, 1972a). The strength of this emission is typical of the young disc population, as extensively discussed by Wilson and Woolley (1970). No emission is visible in the H and K lines of ζ^2 Ret (Hearnshaw, 1975; this work).

In an attempt to improve the understanding of the nature of these stars, we have performed a detailed analysis from observational data obtained under the same conditions for both stars. Section 2 presents the observations and the data reduction; Sect. 3 describes the method of analysis and the results, and these are discussed in the concluding section, where we also suggest some possible solutions to the above problems.

Table 1. Magnitudes of ζ^1 and ζ^2 Ret in the Johnson photometric system

	ζ^1 Ret		ζ^2 Ret	
	Data	T_{eff}	Data	T_{eff}
HD	20766	–	20807	–
HR	1006	–	1010	–
V	5.54	($M_V = 5.47$)	5.24	($M_V = 5.03$)
π	0.097	($M_{\mathrm{bol}} = 5.47$)	0.091	($M_{\mathrm{bol}} = 5.07$)
$U-V$	0.70	5900	0.60	6000
$B-V$	0.64	5730	0.60	5770
$V-R$	0.54	5660	0.49	5930
$V-I$	0.88	5700	0.83	5820
$V-J$	1.12	5715	1.07	5825
$V-H$	1.43	–	1.34	–
$V-K$	1.53	5600	1.42	5800
$V-L$	1.55	5870	1.47	5975
$V-M$	1.41	5810	1.28	6020

References:
From HD to $(V-I)$: Hoffleit and Jaschek (1982)
From $(V-J)$ to $(V-M)$: Koornneef (1983)
Effective temperatures and bolometric corrections: Johnson (1966)

Send offprint requests to: R. Foy

* Based on observations collected at European Southern Observatory, La Silla (Chile)

© European Southern Observatory • Provided by the NASA Astrophysics Data System

1987A&A...177..204D

Table 2. Equivalent widths W of lines measured in the spectrum of ζ^1 and ζ^2 Ret: wavelength LBDA (in Å), multiplet MUL, excitation potential KIEX (in eV), and $-\log(W/\lambda) = -LW/L$ for ζ^1 and ζ^2 Ret

λ (Å)	Mult.	χ_{ex} (eV)	$-\log(W/\lambda)$ ζ^1 Ret	$-\log(W/\lambda)$ ζ^2 Ret	λ (Å)	Mult.	χ (eV)	$-\log(W/\lambda)$ ζ^1 Ret	$-\log(W/\lambda)$ ζ^2 Ret
		NA1					NA1		
4423.27	16	2.10	5.11	5.13	4751.83	11	2.10	5.45	5.45
4494.19	15	2.10		5.81	5682.65	6	2.10	4.86	4.79
4497.68	15	2.10	5.11	5.25	6154.23	5	2.10	4.89	4.82
4664.79	12	2.10	4.93	4.98	6160.75	5	2.10	5.05	5.11
4668.57	12	2.10	5.00	5.08					
		MG1					MG1		
4571.10	1	0.0	4.65	4.64	5785.29	24	5.11	5.49	5.44
5528.42	9	4.33	4.44	4.35	6318.71	23	5.11		5.43
5711.09	8	4.33	4.86	4.87	6319.24	23	5.11	5.27	5.27
		AL1					AL1		
6698.67	5	3.14	4.96	5.20					
		SI1					SI1		
4449.93	0	4.95	5.66	5.86	5684.49	11	4.95	4.90	4.91
4601.27	0	5.08	5.57		6125.03	30	5.61	5.16	5.22
4747.98	0	4.93	5.62	5.59	6142.49	30	5.62	4.98	5.43
4755.26	0	4.92	5.69	5.78	6155.14	29	5.59	4.76	4.91
4792.32	0	4.95	5.32	5.27	6237.33	28	5.61	5.02	5.03
5517.55	0	5.08	5.38	5.38	6243.82	28	5.61	5.08	5.14
5665.56	10	4.92	5.26	5.38	6244.12	28	5.61	5.59	5.59
5666.69	0	5.61	5.88		6244.48	27	5.61	5.11	5.12
5669.75	0	5.62		5.94	6244.48	27	5.61	5.11	5.12
		SI2					SI2		
6347.10	2	8.12	5.43	5.38					
		CA1					CA1		
4506.61	24	2.52	5.48	5.86	6162.18	3	1.89	4.49	4.45
4507.39	24	2.51	5.60	5.63	6163.75	20	2.52	5.00	5.00
4507.80	24	2.52	5.51	5.67	6166.44	20	2.51	4.89	5.00
4509.45	24	2.52	5.60	5.56	6169.04	20	2.52	4.71	4.79
4512.30	24	2.51	5.29	5.29	6169.56	20	2.52	4.77	4.74
4578.60	23	2.51	4.79	4.79	6318.61	27	4.43		5.57
5857.46	47	2.93	4.71	4.73	6439.08	18	2.51	4.57	4.67
6122.22	3	1.88	4.46	4.52	6493.79	18	2.51	4.68	4.77
6156.03	20	2.52	5.64	5.64	6499.65	18	2.51	4.89	4.92
6161.30	20	2.51	5.02	4.98					
		SC1					SC1		
4743.82	14	1.45	5.59	5.62	5671.83	12	0.0	5.03	5.60
4753.18	5	0.0	5.78	5.62					
		SC2					SC2		
4670.41	55	1.36	4.92	4.86	5667.15	29	1.50	5.28	5.27
5239.82	26	1.45	4.89	4.96	5669.04	29	1.49	5.40	5.24
5318.36	22	1.36	5.71	5.64	5684.20	29	1.51	5.27	5.33
5526.82	31	1.76	4.59	4.82	6245.62	28	1.51	5.18	5.15
5657.88	29	1.51	4.99	5.07	6245.62	28	1.51	5.18	5.15
		TI1					TI1		
4417.29	161	1.89	4.94	4.91	4742.12	202	2.15		5.73
4421.76	218	2.24	5.20	5.36	4742.29	111	1.46	5.69	5.89
4422.83	78	1.07	5.06	5.36	4742.80	233	2.24	5.21	5.30
4449.15	160	1.89	4.77	4.85	4747.68	233	2.25	5.78	5.95
4450.90	160	1.87	4.87	5.00	4758.10	233	2.24	5.06	5.06
4453.32	113	1.43	4.77	4.84	4758.92	41	0.84	5.83	5.73
4453.70	160	1.87	4.96	5.04	4759.28	233	2.25	5.06	5.08

Table 2 (continued)

λ (Å)	Mult.	χ_{ex} (eV)	$-\log(W/\lambda)$ ζ^1 Ret	$-\log(W/\lambda)$ ζ^2 Ret	λ (Å)	Mult.	χ (eV)	$-\log(W/\lambda)$ ζ^1 Ret	$-\log(W/\lambda)$ ζ^2 Ret
		TI1					TI1		
4465.80	146	1.73	5.03	5.11	4759.67	202	2.17	5.89	5.53
4471.20	146	1.73	4.89	5.02	4769.80	233	2.25	5.48	5.56
4492.54	184	2.10	5.86	5.33	4771.09	41	0.83	5.32	5.46
4496.17	146	1.75	4.88	5.05	4771.09	41	0.83		5.46
4508.01	0	2.78	5.67		4778.26	232	2.24	5.37	5.48
4512.75	42	0.83	4.85	4.85	4781.72	41	0.85	5.48	5.59
4515.60	184	2.12	5.60	5.76	4792.21	40	0.81	5.62	5.83
4522.81	42	0.82	4.80	4.79	4796.19	260	2.33	5.41	5.48
4534.80	42	0.83	4.67	4.68	4797.98	260	2.33	5.70	5.78
4555.50	42	0.83	4.86	4.90	4805.42	260	2.34	5.25	5.51
4559.93	115	3.54	5.32	5.33	4808.55	305	3.06	5.28	5.38
4562.64	7	0.02	5.48	5.54	4812.24	260	2.34	5.59	
4563.43	266	2.43	5.60	5.51	4812.89	41	0.85	5.62	5.59
4576.52	266	2.33		5.37	4820.41	126	1.50	5.06	5.23
4617.30	145	1.73	4.91	4.93	4821.29	201	2.16	5.89	5.89
4635.56	261	2.33	5.82	5.77	4836.12	241	2.27	5.59	
4656.05	145	1.75	5.47	5.64	4840.88	53	0.90	4.91	4.93
4656.47	6	0.0	4.84	4.87	4880.94	201	2.15	5.70	5.74
4667.59	6	0.02	4.84	4.89	4882.34	231	2.25	5.66	5.74
4668.38	77	1.05	5.95	5.82	5238.57	183	0.85	5.42	5.75
4675.11	77	1.07	5.13	5.12	5247.30	183	2.10	5.38	5.40
4690.80	76	1.07	5.82	5.73	5471.21	106	1.44	5.38	5.62
4693.67	6	0.02	5.43	5.50	5514.35	106	1.43	4.92	5.05
4696.93	203	2.15	5.77	5.88	5514.54	106	1.44	5.42	5.44
4722.61	75	1.05	5.41	5.47	6091.18	238	2.27	5.51	5.63
4733.43	202	2.16	5.78	5.78					
		TI2					TI2		
4417.70	40	1.17	4.56	4.55	4549.82	39	1.18	5.32	5.25
4418.35	51	1.23	4.67	4.67	4552.29	30	1.12	5.37	5.28
4422.00	93	2.05	5.03	5.04	4563.80	50	1.23	4.57	4.54
4443.80	19	1.08	4.49	4.49	4568.33	60	1.22	5.22	5.16
4444.56	19	1.12	4.77	4.79	4571.98	82	1.56	4.54	4.52
4450.50	19	1.08	4.67	4.67	4583.40	39	1.17	5.29	5.17
4464.46	40	1.17	4.79	4.80	4590.00	50	1.23	4.73	4.71
4468.50	31	1.12	4.47	4.49	4609.30	39	1.18	5.52	5.54
4469.16	18	1.08	4.86	4.93	4636.32	38	1.16	5.49	5.40
4470.90	40	1.17	4.76	4.80	4657.20	59	1.24	4.98	5.00
4488.33	115	3.12	4.94	4.94	4662.76	38	1.18	5.38	5.42
4493.53	18	1.08	5.08	5.13	4719.51	59	1.24	5.88	5.65
4501.28	31	1.12	4.55	4.55	4762.78	17	1.08	5.34	5.19
4506.75	30	1.13	5.67	5.53	4798.54	17	1.08	5.06	5.06
4524.69	60	1.23	5.17	5.21	4805.10	92	2.05	4.70	4.69
4533.97	50	1.24	4.56	4.56	4808.29	17	1.08	5.48	5.48
4544.01	60	1.23	5.10	5.14	4821.00	29	1.12	5.78	
4545.14	30	1.13	5.01	4.98	4874.01	114	3.10	5.19	5.16
		VI					VI		
4416.48	22	0.27	4.92	4.94	4635.18	4	0.07	5.82	5.94
4419.94	21	0.28	5.86	5.75	4666.11	94	1.89	5.34	5.34
4421.57	22	0.28	4.98	5.09	4721.53	108	1.95	5.78	
4444.22	21	0.27	4.94	5.10	4758.73	51	1.22	5.56	5.69
4452.01	87	1.87	5.17	5.29	4776.49	128	2.38	5.50	5.62
4468.00	87	1.85	5.56	5.75	4796.91	113	2.10	5.66	5.70
4468.75	102	1.87	5.31	5.59	4807.53	113	2.12	5.62	5.83
4501.99	62	1.38	5.53	5.86	4875.49	3	0.04	5.02	5.18
4514.19	110	1.94	4.95	4.92	4880.53	50	1.19	5.51	5.57
4524.22	99	1.89	5.71	5.63	4881.56	3	0.07	4.96	5.01
4550.72	109	1.95	5.57	5.71	5657.45	37	1.06	5.83	

© European Southern Observatory • Provided by the NASA Astrophysics Data System

1987A&A...177..204D

Table 2 (continued)

λ (Å)	Mult.	χ_{ex} (eV)	−log (W/λ) ζ^1 Ret	−log (W/λ) ζ^2 Ret	λ (Å)	Mult.	χ (eV)	−log (W/λ) ζ^1 Ret	−log (W/λ) ζ^2 Ret
		V1					VI		
4577.18	4	0.0	5.18	5.24	5668.37	37	1.08		5.83
4578.73	109	1.94	5.49	5.46	5670.86	36	1.08		5.67
4580.41	4	0.02	5.15	5.15	6081.45	34	1.05	5.33	5.91
4594.13	4	0.07	4.99	5.02	6090.22	34	1.06	5.36	5.45
4609.66	61	1.38		5.54	6119.53	34	1.06	5.98	5.70
4619.78	4	0.04	5.61		6243.11	19	0.30		5.27
		V2					V2		
4464.34	199	3.76	5.36	5.45	4813.97	197	3.76	5.59	5.59
4558.47	212	3.80			4883.44	209	3.79	5.70	5.60
4564.58	56	2.27	5.37	5.35	4884.05	197	3.76		5.67
		CR1					CR1		
4465.36	127	3.01	5.24	5.31	4600.75	21	1.00	4.77	4.76
4467.56	127	3.01	5.26	5.45	4601.02	32	2.54	5.20	5.20
4491.66	95	2.90	5.25	5.56	4601.14	172	3.12		5.72
4491.85	83	2.99	5.41	5.80	4613.37	21	0.96	4.84	4.86
4492.30	197	3.36	5.15	5.33	4614.73	196	3.37	5.72	5.72
4495.27	275	4.10	5.43	5.93	4616.14	21	0.98	4.74	
4496.86	10	0.94	4.53	4.60	4656.19	147	3.09	5.47	5.42
4498.73	81	2.91	5.25	5.37	4663.32	186	3.10	4.86	4.92
4501.78	81	2.91	5.18	5.26	4663.82	186	3.11	5.17	5.33
4506.84	288	4.18		5.63	4665.91	233	3.55	5.14	5.21
4510.00	0	4.53	5.86		4666.20	99	2.97	5.38	5.38
4510.71	150	3.10	4.95	4.99	4666.48	186	3.14	5.16	5.11
4511.90	150	3.07	5.07	5.11	4669.32	186	3.17	5.23	5.40
4513.22	150	3.09		5.93	4693.95	99	2.98	5.25	5.33
4540.51	33	2.53	4.92	4.98	4695.15	99	2.98	5.50	5.55
4541.07	33	2.53	5.19	5.41	4697.06	62	2.71	5.28	5.26
4554.83	173	3.11	5.81	5.81	4697.40	195	3.37	5.52	5.73
4556.14	173	3.11	4.71	4.68	4722.75	195	3.37	5.95	6.25
4563.24	246	3.85	5.71	5.71	4724.41	145	3.09	5.22	5.41
4564.17	312	4.78	5.60	5.41	4737.35	145	3.09	5.00	4.98
4571.68	32	2.54	5.10	5.03	4745.31	61	2.71	5.56	5.45
4575.11	196	3.37	5.64	5.60	4755.12	124	3.01	5.78	5.73
4578.33	246	3.85	5.94		4756.10	145	3.09	4.90	4.91
4580.06	10	0.94	4.83	4.85	4757.31	290	4.24	5.83	5.65
4587.88	125	3.01		5.87	4759.93	169	3.11		5.95
4591.40	21	0.96	4.80	4.80	4761.25	169	3.12	5.83	5.62
4593.83	190	3.32	5.57	5.57	4770.68	124	3.01	5.65	5.83
4595.05	190	3.32		5.87	4775.13	230	3.55	5.66	6.26
4595.59	286	4.18	5.40	5.29	4789.34	31	2.53	4.93	4.93
		CR1					CR1		
4801.03	168	3.12	5.04	5.09	4953.73	166	3.12	5.00	5.52
4804.65	61	2.71		6.14	4954.81	166	3.11	5.52	5.39
4805.25	283	4.17		5.96	5243.36	201	3.39		5.51
4806.29	61	2.71	5.48	5.48	5247.57	18	0.96	5.11	5.07
4810.26	0	4.53	5.83	5.96	5318.78	225	3.44	5.50	5.64
4810.73	144	3.08	5.83	5.46	5781.76	188	3.32	4.91	5.17
4814.27	144	3.09	5.56	5.70	5783.07	188	3.32	5.44	5.49
4816.13	0	4.53	5.78	5.96	5783.87	188	3.32	5.68	6.02
4816.44	283	4.19	5.66	5.84	5784.98	188	3.32		5.42
4836.86	144	3.10	5.51	5.48	6362.88	6	0.94	5.19	5.39
4874.65	167	3.11	5.74	5.70					
		CR2					CR2		
4555.00	44	4.05	5.03	4.97	4836.24	30	3.86	5.31	5.26
4558.70	44	4.05	4.78	4.74	4836.24	30	3.86	5.31	5.26
4588.20	44	4.05	4.87	4.80	4876.40	30	3.85	5.00	4.97
4592.10	44	4.05	5.02	5.00	4952.84	0	6.28	5.37	5.71
4616.60	44	4.05	5.12	5.03	5237.33	43	4.05	5.24	5.09
4812.35	30	3.86	5.26	5.22	5246.78	23	3.71	5.57	

Table 2 (continued)

λ (Å)	Mult.	χ_{ex} (eV)	−log (W/λ) ζ^1 Ret	−log (W/λ) ζ^2 Ret	λ (Å)	Mult.	χ (eV)	−log (W/λ) ζ^1 Ret	−log (W/λ) ζ^2 Ret
		MN1					MNI		
4451.59	22	2.89	4.66	4.71	4761.50	21	2.94	4.86	4.87
4453.00	22	2.93	4.90	5.03	4762.37	21	2.89	4.66	4.68
4464.77	22	2.92	4.52	4.57	4838.22	43	3.86	5.90	5.90
4470.10	22	2.93	4.84	4.94	5470.64	4	2.64	4.97	5.09
4493.90	22	2.94	4.91	4.99	5516.82	4	2.18	5.40	5.46
4502.22	22	2.92	4.86	4.95	6013.50	27	3.07	5.01	4.99
4571.69	21	2.89	5.52	5.52	6016.65	27	3.07	4.62	4.85
4739.11	21	2.94	4.98	5.04	6021.80	27	3.07	4.85	4.85
4754.00	16	2.27	4.57	4.58					
		FE1					FE1		
4419.27	893	3.63	5.29	5.50	4487.75	594	3.24	5.33	5.50
4419.78	644	5.39	5.30	5.45	4488.13	819	3.60	4.85	4.94
4420.28	0	0.0	5.10	5.18	4489.70	2	0.12	4.60	4.64
4423.14	412	4.87	4.92	5.04	4490.09	469	3.02	4.71	4.77
4442.84	69	2.18	4.79	4.83	4492.70	969	3.93	4.99	5.11
4443.20	350	2.85	4.56	4.58	4493.38	796	3.57	5.63	
4445.48	2	0.09	4.98	5.11	4494.06	973	3.98	5.14	5.15
4446.80	828	3.67	4.75	4.81	4494.60	68	2.19	4.36	4.35
4447.70	68	2.21	4.42	4.46	4495.58	827	3.60	5.15	5.33
4448.95	891	3.64	5.50	5.53	4495.96	825	3.65	4.93	5.02
4450.32	476	3.11	4.88	4.96	4498.56	988	3.88	5.59	5.75
4450.76	972	3.88	5.23	5.29	4500.64	0	0.0	5.41	5.75
4452.62	969	3.94	5.17	5.36	4502.60	796	3.57	5.14	5.35
4466.17	901	3.64	5.38	5.71	4507.23	474	3.11		5.60
4466.94	992	3.93	4.71	4.79	4510.83	823	3.60	5.53	5.71
4469.38	830	3.64	4.56	4.60	4511.07	970	3.94	5.81	5.81
4471.68	2	0.11	5.31	5.50	4513.72	514	3.05	5.71	5.56
4472.72	900	3.64	4.60	4.71	4515.18	319	2.87	5.51	5.87
4483.70	830	3.67	4.69	4.74	4523.40	829	3.64	5.04	5.07
4485.98	825	3.65	5.24	5.56	4525.15	819	3.62	4.62	4.62
4487.37	824	3.60	5.48	5.67	4541.32	640	3.25	5.35	5.51
		FE1					FE1		
4541.94	593	3.27	5.48	5.60	4741.08	688	3.33	5.24	5.25
4542.43	894	3.64	5.05	5.10	4741.50	346	2.82	4.85	4.85
4544.49	970	3.98	5.81		4742.94	1072	4.19	5.83	5.73
4550.77	0	0.0	4.81	4.79	4744.12	1168	4.39		5.73
4551.65	972	3.94	5.25	5.30	4744.64	17	0.99	5.69	5.69
4554.46	319	2.86	5.12	5.12	4745.14	67	2.22	5.62	5.41
4556.94	638	3.26	5.28	5.37	4749.26	1098	4.26	5.62	5.62
4560.10	823	3.61	5.10	5.06	4749.96	1206	4.56	5.20	5.16
4564.70	823	3.65	5.28	5.32	4760.07	384	3.04	5.62	5.69
4564.83	472	3.07	5.27	5.30	4773.53	408	3.02	5.83	5.96
4568.80	554	3.26	4.86	4.90	4776.07	521	3.30	5.27	5.39
4571.44	319	2.87	5.51	5.51	4779.44	720	3.41	5.08	5.13
4572.86	819	3.65	5.44	5.46	4780.81	633	3.25	5.56	5.66
4574.24	554	3.20	5.14	5.14	4787.83	384	3.00	5.07	5.11
4574.73	115	2.28	4.96	4.97	4788.80	588	3.22	4.88	4.87
4579.82	469	3.07	5.42	5.44	4789.66	753	3.53	4.79	4.79
4580.59	827	3.65	5.08	5.05	4790.56	1068	4.15	5.69	5.78
4582.95	384	2.84	5.94	5.44	4790.75	632	3.25	5.66	5.74
4587.72	971	3.98	5.54	5.68	4791.21	633	3.27	4.94	4.99
4592.51	39	1.56	4.47	4.46	4798.27	1042	4.19	5.12	5.10
4593.50	971	3.95	5.27	5.24	4798.74	38	1.61	5.26	5.32
4596.07	820	3.60	4.74	4.75	4799.07	1098	4.28	5.78	5.66
4600.94	591	3.24	5.44	5.57	4799.41	388	3.64	5.17	5.22
4606.01	893	3.64		6.02	4800.13	384	3.04	5.51	5.74
4607.09	724	3.41	5.72	6.12	4801.61	1115	4.28	5.62	5.89
4612.61	349	2.83	5.68	5.68	4802.52	1206	4.61	5.56	5.53
4613.21	554	3.29	4.86	4.87	4804.52	794	3.57		5.41
4619.30	821	3.63	4.76	4.77	4805.55	1207	4.64	5.96	5.51
4620.13	468	3.07	5.72	5.77	4807.72	688	3.37	5.04	5.12

© European Southern Observatory • Provided by the NASA Astrophysics Data System

1987A&A...177..204D

Table 2 (continued)

λ (Å)	Mult.	χ_{ex} (eV)	−log (W/λ) ζ^1 Ret	−log (W/λ) ζ^2 Ret	λ (Å)	Mult.	χ (eV)	−log (W/λ) ζ^1 Ret	−log (W/λ) ζ^2 Ret
		FE1					FE1		
4635.62	319	2.86	5.64	5.82	4808.16	633	3.25	5.23	5.32
4635.85	349	2.84	4.97	5.01	4809.15	933	5.66	5.59	5.66
4636.68	513	3.05	5.68	5.94	4809.94	793	3.57	5.48	5.44
4657.59	346	2.84	5.22	5.31	4811.05	467	3.07	5.53	5.53
4658.30	591	3.27	5.40	5.47	4813.12	630	3.27	5.38	5.36
4661.50	1207	4.54	5.16	5.21	4813.72	1243	4.58		5.74
4661.98	409	2.99	5.03	5.07	4814.37	0	0.0	5.74	5.89
4665.55	1044	4.07	5.58	5.49	4815.25	720	3.41	5.32	5.48
4667.46	822	3.60	4.78	4.72	4816.68	588	3.27	5.84	6.04
4668.12	554	3.26	4.59	4.58	4818.66	719	3.41	5.78	
4669.18	821	3.65	4.84	4.85	4835.87	1068	4.10	5.01	5.07
4672.04	1045	4.14	5.73		4837.67	1243	4.58	5.90	
4672.84	40	1.61	5.13	5.15	4838.09	630	3.25	5.63	5.96
4673.17	820	3.65	4.65	4.66	4838.52	687	3.42	4.96	4.92
4677.60	1072	4.15	5.61	5.52	4838.83	1167	4.43	5.79	6.26
4690.14	820	3.69	4.97	4.94	4839.55	588	3.27	4.93	4.94
4690.38	17	1.01	5.61	5.55	4839.78	1206	4.61	5.70	
4720.58	1114	4.21	5.88	5.88	4840.30	1068	4.15	4.80	4.84
4733.60	38	1.48	4.76	4.80	4873.75	633	3.30	5.40	5.42
4734.11	1133	4.29	5.17	5.21	4874.36	467	3.07	5.36	5.36
4735.85	1042	4.07	4.90	4.92	4875.35	1038	4.19		5.90
4736.80	554	3.20	4.54	4.57	4875.74	1243	4.59		6.04
4737.63	590	3.27	5.19	5.25	4875.88	687	3.36	4.92	5.00
4740.34	409	3.02	5.14	5.18	4876.20	631	3.25	5.63	
		FE1					FE1		
4882.15	687	3.40	4.86	4.89	6020.19	1178	4.61	5.08	5.05
4923.15	0	0.0	5.37	5.43	6082.72	64	2.22	5.16	5.29
4924.78	114	2.27	4.73	4.81	6089.57	1327	5.02	5.02	5.43
4952.65	1111	4.21		5.09	6093.65	1177	4.61	5.26	5.30
4954.29	1093	4.81	5.80	5.85	6120.25	14	0.91	5.92	6.05
5242.50	843	3.62	4.78	4.88	6157.73	1015	4.06	5.02	5.02
5243.78	1089	4.26	4.71	4.93	6165.36	1018	4.14	5.24	5.15
5247.06	1	0.09	5.18	5.14	6240.65	64	2.22	5.30	5.27
5320.04	877	3.64	5.33	5.64	6246.33	816	3.59	4.80	4.71
5321.11	1165	4.43	5.18	5.10	6318.03	168	2.44	4.65	4.77
5322.05	112	2.27	4.89	4.93	6322.69	207	2.58	5.00	4.93
5401.27	1146	4.32	5.14	5.13	6430.85	62	2.18	4.78	4.87
5470.09	1144	4.44	5.25	5.28	6430.85	62	2.18	4.78	4.87
5473.17	1064	4.19	5.28	5.31	6494.50	1225	4.73	5.24	5.19
5473.91	1062	4.14	4.81	4.86	6494.99	168	2.40	4.68	4.66
5525.58	1062	4.21	5.02	5.02	6494.99	168	2.40	4.68	4.66
5784.67	686	3.40	5.05	5.09	6496.47	1258	4.79	4.97	5.03
5855.09	1179	4.61	5.56	5.51	6498.95	13	0.96	4.89	5.16
5856.10	1128	4.29	5.23	5.34	6699.14	1228	4.59	5.57	5.43
		FE2					FE2		
4416.83	27	2.78	4.65	4.67	4658.04	170	5.57	5.68	5.82
4446.24	187	5.95	5.56		4661.15	170	5.57	5.88	
4472.93	37	2.84	5.06	5.01	4663.18	754	5.75	5.45	5.47
4489.16	37	2.83	4.63	4.67	4663.71	44	2.89	5.34	5.18
4491.40	37	2.83	4.75	4.80	4666.75	37	2.83	5.03	4.95
4508.30	38	2.83	4.78	4.73	4670.17	25	2.58	5.28	5.19
4515.34	37	2.83	4.79	4.71	4720.13	54	3.20	5.83	
4534.17	37	2.85	5.06	5.05	4840.00	30	2.68	5.56	5.51
4541.32	640	3.25		5.51	4923.93	42	2.88	4.54	4.51
4541.52	38	2.85	4.86	4.83	4954.02	168	5.57	5.85	5.64
4555.90	37	2.83	4.77	4.75	5525.14	56	3.27	5.13	5.29
4576.30	38	2.83	4.93	4.91	6084.11	46	3.20	5.41	5.53
4582.83	37	2.83	5.02	4.97	6238.39	74	3.87	5.18	5.18
4595.69	38	2.85	5.87	5.87	6239.95	74	3.89	5.93	5.68

Table 2 (continued)

λ (Å)	Mult.	χ_{ex} (eV)	−log (W/λ) ζ^1 Ret	−log (W/λ) ζ^2 Ret	λ (Å)	Mult.	χ (eV)	−log (W/λ) ζ^1 Ret	−log (W/λ) ζ^2 Ret
		FE2					FE2		
4601.38	43	2.89	5.82	5.40	6247.56	74	3.89	4.99	5.04
4620.50	38	2.83	5.03	4.99	6247.56	74	3.89	5.04	4.99
4635.31	186	5.95	5.64	5.36	6432.68	40	2.88	5.25	5.42
4656.98	43	2.89	5.17	5.12					
		CO1					CO1		
4417.41	150	3.07	5.32	5.29	4749.66	156	3.05	5.14	5.23
4421.33	150	2.39	5.18	5.34	4754.36	156	3.23	5.62	5.62
4445.68	150	3.10	5.62	5.66	4756.73	0	3.93		5.62
4469.56	150	2.96	5.23	5.45	4781.45	57	1.88	5.48	5.66
4471.56	150	3.07	5.27	5.48	4795.84	185	3.95	5.62	5.56
4543.81	142	2.71	5.30	5.37	4796.37	14	0.43		5.83
4580.15	27	0.92	5.64	5.46	4813.48	158	3.21	5.07	5.15
4594.64	176	3.63	5.20	5.51	4882.71	158	3.25	5.66	5.63
4693.20	156	3.23	5.52	5.45	5399.78	0	4.21	5.46	5.55
4734.83	156	3.25		5.73	5530.79	38	1.79	5.51	5.30
4737.76	57	1.96	5.78		6093.15	37	1.74	5.77	5.86
		NI I					NI I		
4422.97	168	3.68	5.27	5.27	4756.50	98	3.47	4.86	4.84
4450.10	178	3.94	5.80	5.80	4758.43	193	3.85	5.89	5.69
4466.39	168	3.70	5.10	5.29	4762.63	71	1.93	5.03	5.08
4470.50	86	3.38	4.67	4.70	4773.41	167	3.70	5.48	5.50
4501.65	115	3.70	5.53		4790.97	71	1.95	5.56	5.78
4506.33	133	3.54	5.51	5.51	4806.99	163	3.68	4.93	
4513.00	163	3.70	5.45	5.51	4808.88	160	3.70	5.59	5.42
4551.23	236	4.17	5.27	5.25	4811.99	130	3.66	5.31	5.36
4553.17	135	3.66	5.51	5.54	4814.59	98	3.60	5.38	5.48
4606.20	100	3.58	5.07	5.07	4815.93	131	3.54	5.66	5.62
4617.97	115	3.77		5.61	4821.13	254	4.12	5.25	5.40
4620.35	163	3.68	5.94	5.82	4838.65	260	5.03	5.24	5.33
4657.38	254	4.26	5.88		4873.26	112	3.74	5.28	5.36
4664.32	147	3.63	5.68	5.95	4873.45	111	3.68	4.94	4.96
4666.99	146	3.80	5.18	5.23	4874.79	98	3.54	5.57	
4667.77	163	3.70	5.18	5.16	4952.28	113	3.61		5.41
4674.76	0	3.63	5.49	5.49	4953.22	111	3.72	5.41	5.10
4675.60	115	3.61	5.45	5.40	5669.95	250	4.26	5.28	5.42
4723.00	0	4.15	5.73		5682.21	232	4.10	4.97	5.07
4723.35	162	3.68	5.88		5857.76	228	4.17	4.98	4.95
4723.90	167	3.68	6.25	5.88	6086.29	249	4.26	4.83	5.26
4736.51	99	3.48	5.55	5.58	6119.76	244	4.26	5.41	5.67
4740.17	99	3.48	5.53	5.48	6163.42	230	4.10	5.08	5.03
4752.40	132	3.64	4.94	4.98	6322.17	249	4.15		5.52
4754.77	141	3.63	5.12	5.09	6360.82	229	4.17	5.63	5.41
		ZN1					ZN1		
4722.16	2	4.03	4.90	4.89	6362.35	17	5.79	5.24	5.35
4810.53	2	4.06	4.85	4.87					
		SR1					SR1		
4607.30	2	0.0	5.09	5.12	4876.09	4	1.80		5.57
4722.28	5	1.80		5.88					
		Y1					Y1		
4487.26	14	1.37	5.41	5.71	4760.97	4	0.07	5.96	5.65
4487.51	14	1.36	5.59	5.93	4819.64	13	1.36	5.84	
4513.58	15	1.90	5.76		4839.88	13	1.43	5.90	
		Y2					Y2		
4883.69	22	1.08	4.98	4.98	5527.78	12	1.40	5.82	
5402.78	35	1.84	5.55	5.72					

© European Southern Observatory • Provided by the NASA Astrophysics Data System

1987A&A...177..204D

Table 2 (continued)

λ (Å)	Mult.	χ_{ex} (eV)	−log (W/λ) ζ^1 Ret	−log (W/λ) ζ^2 Ret	λ (Å)	Mult.	χ (eV)	−log (W/λ) ζ^1 Ret	−log (W/λ) ζ^2 Ret
		ZR1					ZR1		
4507.10	31	0.54	5.67		4772.31	43	0.62	5.56	6.13
4542.23	49	0.63	5.81		4809.48	0	1.58	5.66	5.89
4739.45	43	0.65	5.65	5.73					
		ZR2					ZR2		
4443.00	88	5.57	5.75	5.86	4494.38	130	5.52	5.37	
4445.85	96	5.62	5.50	5.70	4513.95	67	0.97	5.24	5.23
4485.42	79	5.81	5.53	5.86					
		BA2					BA2		
4524.94	3	2.51	5.13	5.19	6141.73	2	0.70	4.69	4.74
4554.04	1	0.0	4.46	4.45	6496.91	2	0.60	4.70	4.83
5853.69	2	0.60	5.05	4.98					
		LA2					LA2		
4574.90	23	0.17	5.81	5.49	4748.74	65	0.93	5.65	5.95
4619.90	76	1.75		5.82	4809.02	37	0.23	5.74	5.96
4662.51	8	0.0	5.61	5.72					

2. Observations, data reduction

The observations were arried out at the European Southern Observatory (ESO), La Silla (Chile). We have utilized the coudé spectrograph of the 1.52 m telescope. Seven spectrograms per star were obtained in 1972 October, in two spectral ranges. Blue spectrograms (from 3800 Å to 5000 Å) were exposed on baked IIaO Kodak plates, the width being 0.8 mm, the reciprocal dispersion 3.2 Å mm^{-1}, and the resolution 0.14 Å. Yellow spectrograms (from 5000 Å to 6750 Å) were exposed on IIaF Kodak plates, with a width of 0.6 mm, a reciprocal dispersion of 12.4 Å mm^{-1}, and a resolution of 0.30 Å.

The spectrograms and the photometric calibration plates were recorded using the Brückner microphotometer of the Institut d'Astrophysique de Paris; the projected slit was set to 5 μm. Transmissions were converted into relative intensities and then spectrograms were averaged. Equivalent widths were measured from the mean spectrograms, using a line fitting method allowing accurate measurements of weak lines, in order to derive accurate abundances (Foy, 1971). The lines were assumed to have gaussian profiles, with the same FWHM as in the solar spectrum. An analytical profile was fitted to the average one (per short spectral range: 5–25 Å), using a least squares method, the unknown quantities being the central depth of the lines. The list of the lines taken into account in the analytical profiles have been compiled from the solar spectrum (Moore et al., 1966). We have not made use of lines at wavelengths shorter than 4400 Å, because of the difficulty to estimate the spectral continuum at these wavelengths. Most of the lines are more or less blended: our method of equivalent width measurements allows proper corrections for blend effects when the blended portion of their profile is not saturated. Heavily saturated blended lines have been rejected from the list (Table 2).

As the reference solar curves of growth used in this study have been constructed with Moore et al.'s equivalent width $W_\odot$ of the spectrum of the centre of the solar disc, we have corrected the measured equivalent widths $W(3.2)$ of ζ^1 and ζ^2 Ret according to the relation: $W_\odot = 0.88\ W(3.2)$ (Da Silva, 1975), for the 3.2 Å mm^{-1} spectrograms. Equivalent widths measured from 12.4 Å mm^{-1} spectrograms have been corrected so that they lead to the same Fe abundance as determined from 3.2 Å mm^{-1} spectrograms

$$W_\odot = 0.96\, W(12.4) - 7\,\text{mÅ}\,. \tag{1}$$

These relations were derived from spectrograms of the Moon observed with the same equipment as that used for this paper.

3. Method of analysis, results

To analyse the equivalent widths and the Hβ line profiles, we have used model atmospheres scaled from the $T(\tau)$ relationship of Peytremann (1974a, b), as described in Da Silva (1975) and in Kovacs and Foy (1977). Let us briefly recall that these models are in convective/radiative equilibrium, and are computed assuming a plane-parallel atmosphere in LTE. Abundances have been derived using curves of growth, of which the abscissae are written as $\log x + [\Gamma]_\odot^{\text{model}}$ where:

$$\Gamma = \frac{\pi e^2}{m c^2} \int_0^\infty G_\lambda(x)\, P(x)\, dx\,. \tag{2}$$

G_λ is the weighting function for weak lines computed for the integrated stellar disc, $P(x)$ the occupation number of the lower level of the transition divided by the statistical weight, and x is the number of hydrogen atoms contained in a column of one square centimeter cross-section above the running point x. The notation $[\Gamma]_\odot^{\text{model}}$ means $\log \Gamma\,(\text{model}) - \log \Gamma\,(\odot)$.

$\log x_\odot$ values have been derived from the semi-empirical Fe I curve of growth by Foy (1972b), taking into account the splitting in the case of Fe I, and the solar equivalent widths by More et al. (1966).

The effective temperatures T_{eff} and the gravities g have been derived using the "diamond diagram" method discussed in detail by Blanc-Vaziaga et al. (1973) and by Da Silva (1975): in the $\theta_{\text{eff}} = 5040/T_{\text{eff}}$ versus $\log g$ plane, we have determined the loci of points satisfying the following criteria:

– Fit of theoretical Hβ profiles to the observed ones (Fig. 1a, b). Hβ profiles have been computed using a routine by Praderie (1967); we have taken into account only quasi-static broadening, since resonance broadening is negligible for Hβ. We

© European Southern Observatory • Provided by the NASA Astrophysics Data System

1987A&A...177..204D

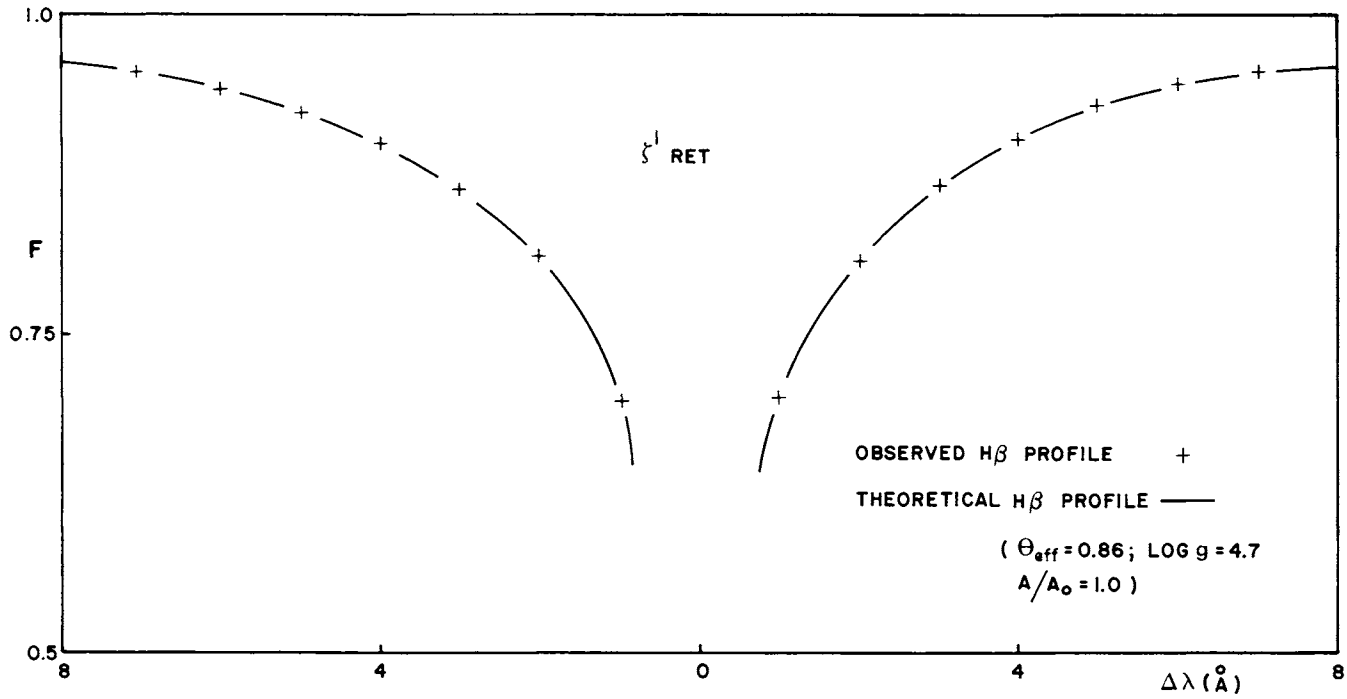

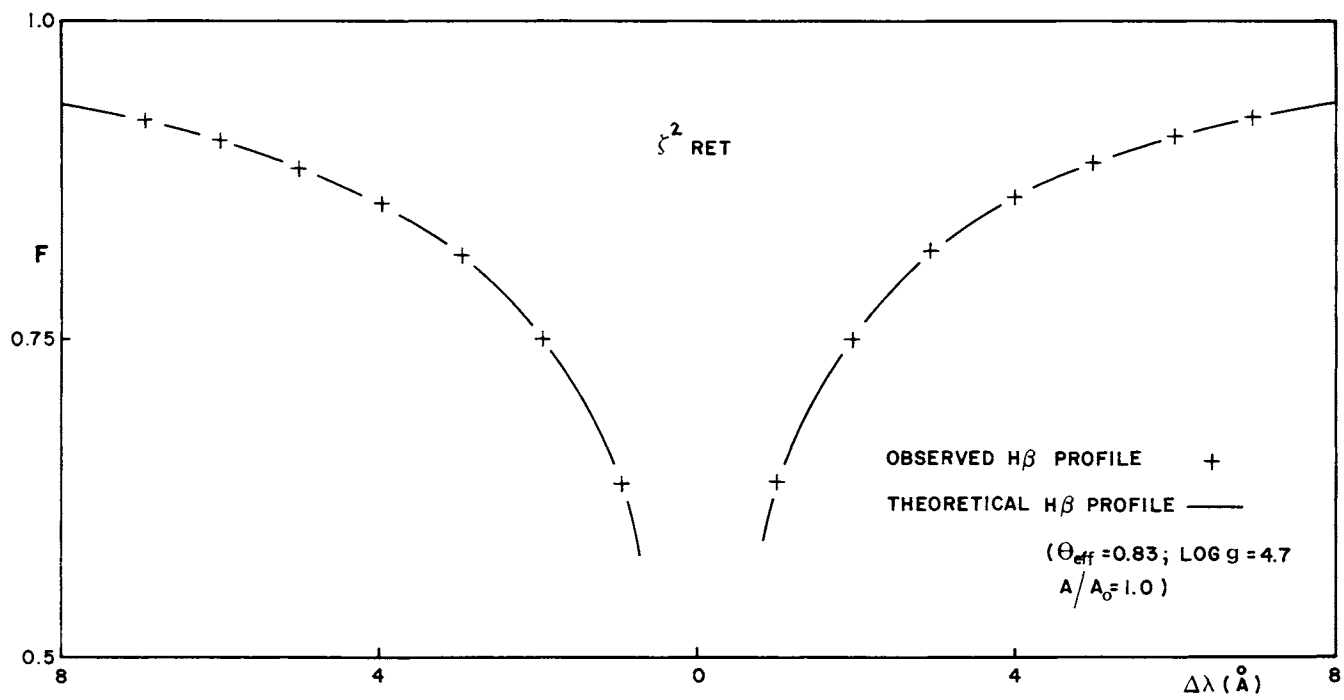

Fig. 1 a and b. Fit of theoretical Hβ profile (solid lines) to the observed ones (crossed). **a** ζ^1 Ret; **b** ζ^2 Ret. $A/A_\odot$ stands for the mean abundance of electron donors relatively to the Sun

have not used Hα profiles because the dependence of Hα on the atmospheric parameters is more complex than that of Hβ in the temperature range which is of importance here (Da Silva, 1975). We have derived $\theta_{\rm eff}(\zeta^1) = 0.86 \pm 0.02$ and $\theta_{\rm eff}(\zeta^2) = 0.83 \pm 0.02$. These determinations almost perfectly agree with those by Gehren (1981) who made use of both Hα and Hβ profiles; he found $\theta_{\rm eff}(\zeta^1) = 0.860$ and $\theta_{\rm eff}(\zeta^2) = 0.837$.

– Ionization equilibrium: a model atmosphere fulfils this condition when both neutral and ionized lines of an element lead to the same abundance of this element; we have applied this to Fe, Ti and Cr.

– Fit of the absolute magnitude; the trigonometric parallaxes are large enough to be reliable: $\pi(\zeta^1) = 0''.097$ and $\pi(\zeta^2) = 0''.091$. We have adopted $\pi(\zeta^1) = \pi(\zeta^2) = 0''.094 \pm 0''.005$, assuming there-

© European Southern Observatory • Provided by the NASA Astrophysics Data System

1987A&A...177..204D

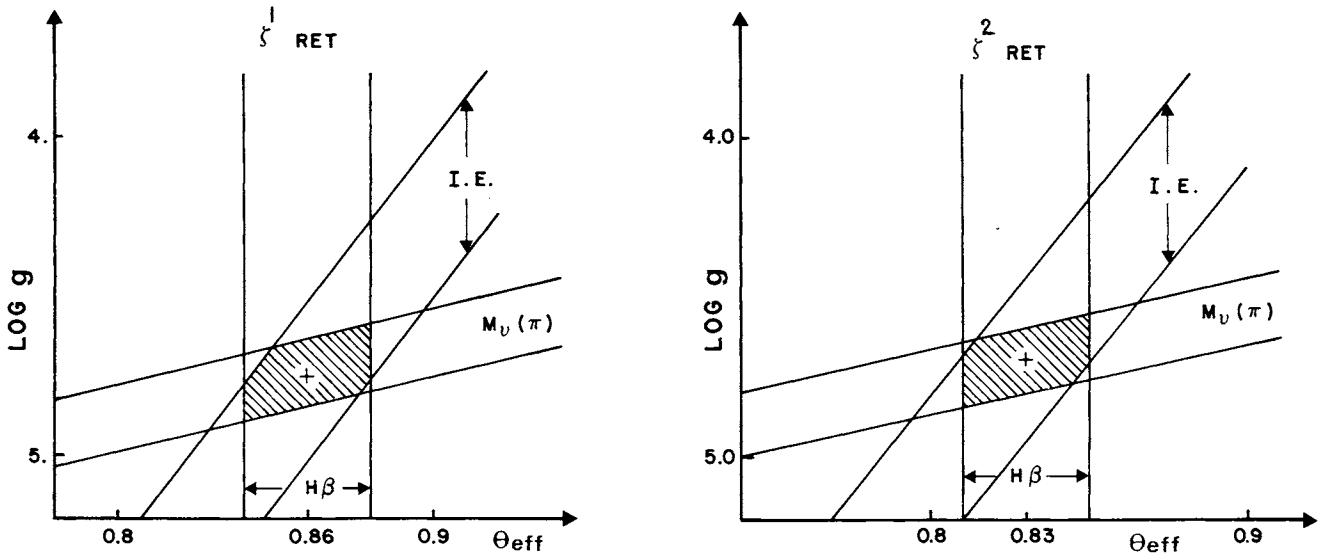

Fig. 2a and b. Loci of models which reproduce the observed Hβ profile (Hβ), the ionization equilibrium (IE), and trigonometric absolute magnitude (M_v), respectively for ζ^1 **a** and ζ^2 **b** Ret

fore that both stars lie at the same distance from the Sun. We have applied to M_v the bolometric correction given by Johnson (1966) to derive $M_{\rm bol}$; then we have used the relation:

$$\log g_* = \log g_\odot - 0.4\,(M_{\rm bol\odot} - M_{\rm bol*}) + \log \mathfrak{M}_*/\mathfrak{M}_\odot + 4 \log T_{\rm eff,*}/T_{\rm eff,\odot}$$

where $\mathfrak{M}$ stands for the stellar mass. For each star, we have computed log g for two values of $T_{\rm eff}$ around the value determined from the Hβ profile, and using the mass derived from the evolutionary tracks by Hejlesen (1980).

Usually near infrared photometric indices are good tracers of the effective temperature. We have not made use of these indices because we have derived different values of $T_{\rm eff}$, depending on the indices.

The three criteria closely intersect around ($\theta_{\rm eff} = 0.86$, $\log g = 4.75$) and ($\theta_{\rm eff} = 0.83$, $\log g = 4.70$), respectively, for ζ^1 and ζ^2 Ret (Fig. 2a and b). We have adopted these parameters to determine the abundances: the iron abundance relative to the Sun is $[{\rm Fe/H}]^{\zeta^1}_\odot = [{\rm Fe/H}]^{\zeta^2}_\odot = +0.1 \pm 0.2$. The error bar quoted is a conservative one: the internal error is much lower, as can be judged from the well populated linear part of the iron curves of growth (Fig. 3a and b). The list of abundances relative to the Sun for 18 elements is given in Table 3.

4. Discussion

The striking result of our detailed analysis is the high gravity of both ζ^1 and ζ^2 Ret: $\log g \simeq 4.7$. It confirms the preliminary analysis by Foy (1972a). The similarity of the peculiarities of ζ^1 and ζ^2 Ret supports the idea that they have a common origin, which is what we shall assume in the following.

The gravity $\log g = 4.7$ is typical of unevolved metal-poor stars. But we have found for both ζ^1 and ζ^2 Ret: $[{\rm Fe/H}]^*_\odot = +0.1$, which is not in conflict with the previous determinations: $[{\rm Fe/H}]^{\zeta^1}_\odot = -0.37$ from a coarse analysis by Danziger (1966), or $[{\rm Fe/H}]^{\zeta^1}_\odot = -0.10$ (Foy, 1972a) and $[{\rm Fe/H}]^{\zeta^2}_\odot = -0.32$ (Hearnshaw, 1975) from detailed analysis, considering the errors in these latter estimates. Thus ζ^1 and ζ^2 Ret are definitely *not* metal-poor.

We shall now discuss some possible solutions to the problem of the apparently conflicting facts that these stars have a high gravity and an ultraviolet excess but are not metal-poor, are old disc population dwarfs yet ζ^1 Ret exhibits emission line in the H and K Ca II lines.

4.1. *An error in the $T_{\rm eff}$ determination*

Adopting a lower effective temperature for ζ^1 and ζ^2 Ret would lead to a lower gravity as determined from the ionization equilibrium conditions. Hearnshaw (1975) has adopted $\theta_{\rm eff} = 0.90$ and $\log g = 4.51$ for ζ^2 Ret; but he has determined log g only from the trigonometric parallax, without checking whether the condition of ionization equilibrium was fulfilled.

In fact, an increase of $\theta_{\rm eff}$ by $\Delta\theta_{\rm eff} = 0.02$ for both stars would restore a "normal" gravity $\log g = 4.5$, with a slight decrease by 0.13 dex in the iron abundance. It does not seem to be allowed neither from our profiles nor from those published by Gehren (1981).

The observed UV excess could be accounted for by $[{\rm Fe/H}]^*_\odot < -0.4$ which would be obtained only if our $\theta_{\rm eff}$ was wrong by 0.1, clearly contradicting the Hβ profile analysis. ζ^1 Ret would then be a subgiant with $\log g < 3.8$, and its spectroscopic absolute magnitude would be at least 2 magnitudes brighter than that derived from the trigonometric parallax, i.e.: the error in the trigonometric parallax should be $\Delta\pi = 0''.12$; this also is out of the range of observational errors.

Therefore an error in the effective temperature cannot be put forward to remove the above discrepancies.

4.2. *Both ζ^1 and ζ^2 Ret are binaries*

It could be that both ζ^1 and ζ^2 Ret are close binaries. Colours would be affected, as well as the spectroscopic analysis. A very close companion of ζ^1 Ret would heat the facing hemisphere of ζ^1 Ret enough to account for the UV excess and for the H and K emission lines. Nevertheless we think this hypothesis is very unlikely, on the basis of the following arguments.

© European Southern Observatory • Provided by the NASA Astrophysics Data System

1987A&A...177..204D

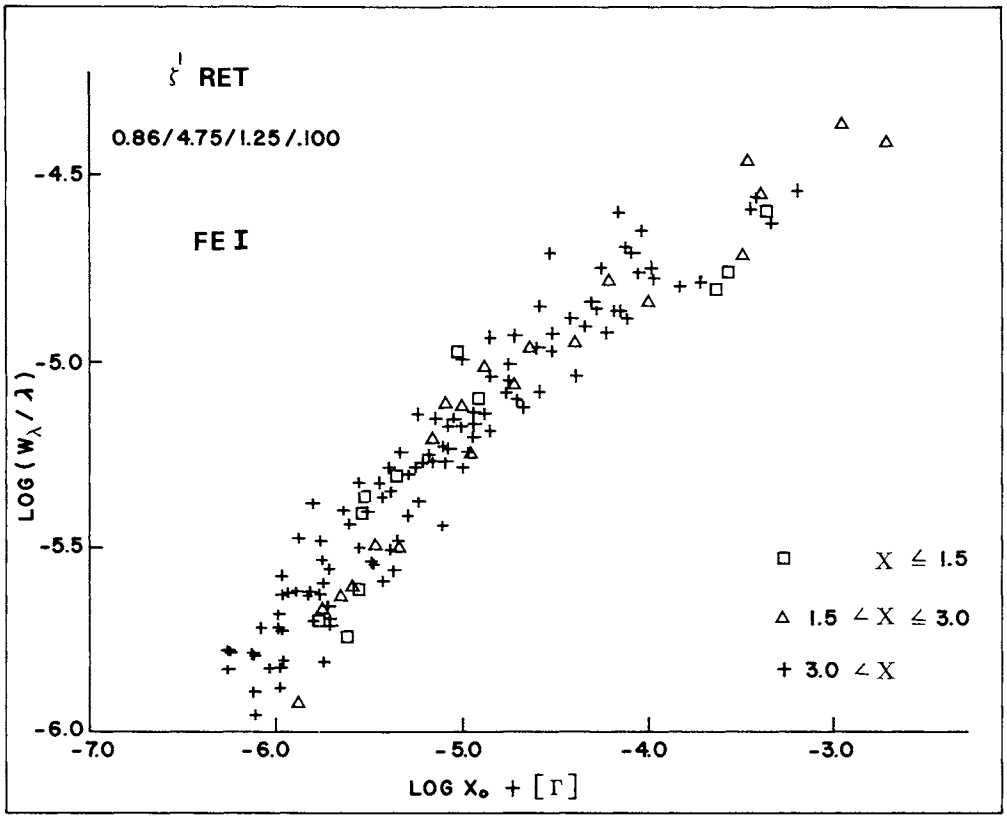

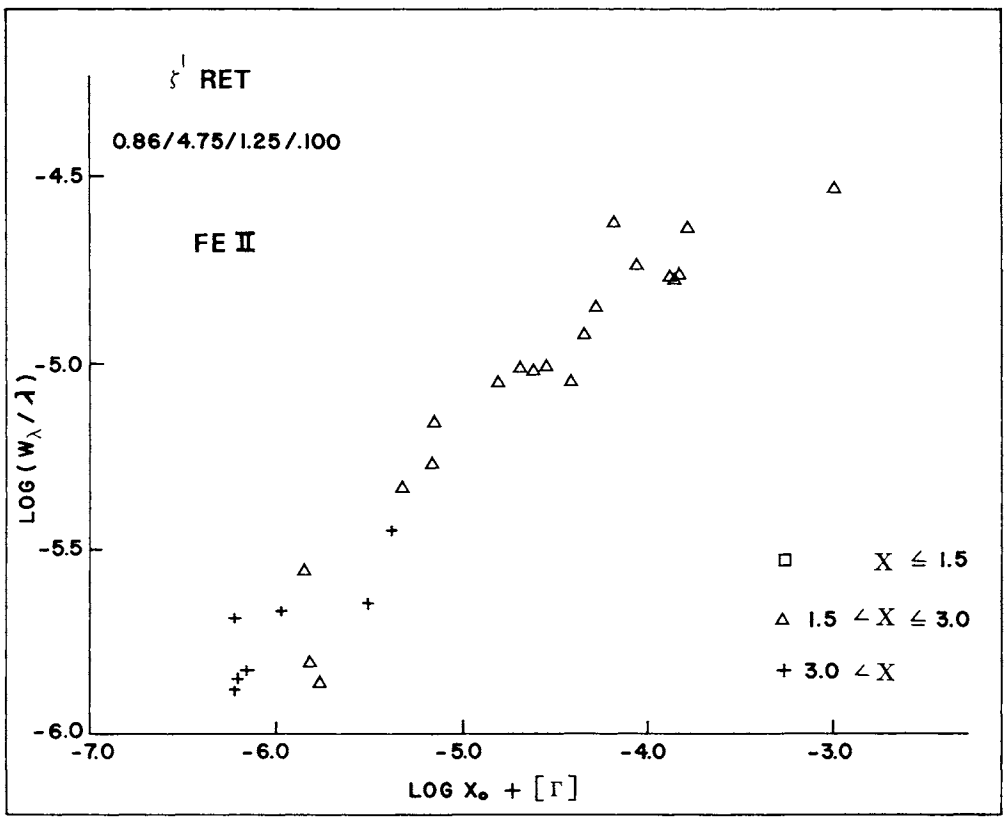

Fig. 3a and b. Curve of growth of iron for: **a** ζ^2 Ret, computed with the model $\theta_{\rm eff}=0.86$, $\log g=4.75$, $[M/H]^{\zeta^1}_{\odot}=+0.1$, $n({\rm He})/n({\rm H})=0.1$. **aI** Fe I; **aII** Fe II. **b** ζ^2 Ret, computed with the model $\theta_{\rm eff}=0.83$, $\log g=4.70$, $[M/H]^{\zeta^2}_{\odot}=+0.1$, $n({\rm He})/n({\rm H})=0.1$. **bI** Fe I; **bII** Fe II. Symbols refer to the excitation potential χ of the lines: □: $\chi \leqq 1.5$ eV +: $3.0 > \chi$. △: $1.5 < \chi \leqq 3.0$ eV

© European Southern Observatory • Provided by the NASA Astrophysics Data System

1987A&A...177..204D

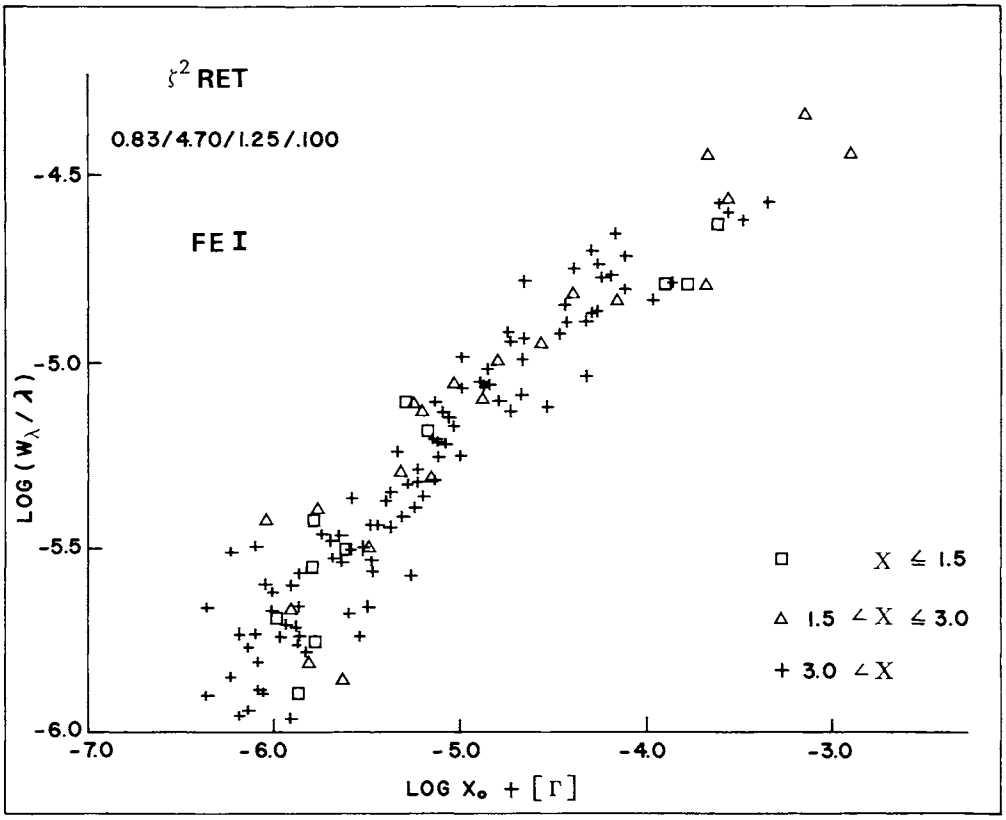

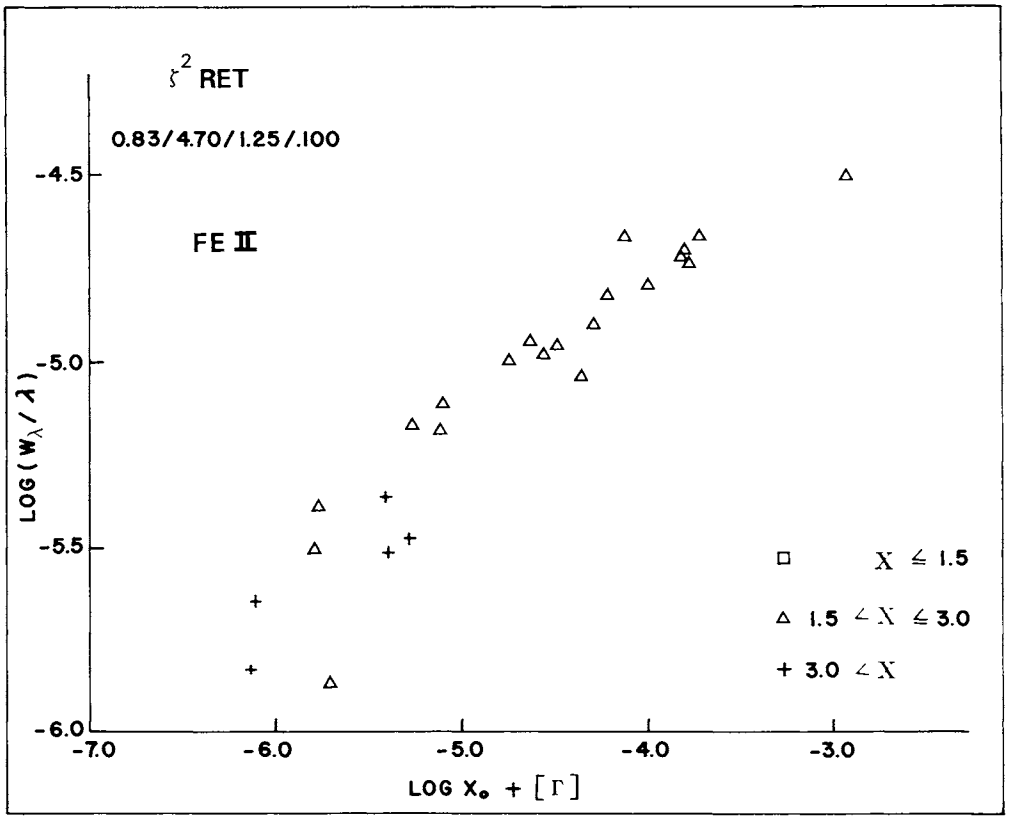

Fig. 3b

© European Southern Observatory • Provided by the NASA Astrophysics Data System

1987A&A...177..204D

Table 3. Logarithmic abundances of heavy elements E/H relative to the Sun in ζ^1 and ζ^2 Ret. N: number of lines used for the curve of growth of each elements

Element	ζ^1 Ret		ζ^2 Ret	
	[E/H]	N	[E/H]	N
Na I	0.13	8	0.16	9
Mg I	−0.20	5	−0.1	6
Al I	1.0	1	0.6	1
Si I	0.16	17	0.10	17
Ca I	0.16	29	0.13	29
Sc I	0.50	3	0.40	3
Sc II	0.10	10	0.10	10
Ti I	0.13	64	0.16	63
Ti II	0.20	36	0.13	35
V I	0.20	31	0.20	32
V II	0.30	4	0.23	5
Cr I	0.10	49	0.10	46
Cr II	0.04	12	0.07	12
Mn I	0.10	17	0.0	17
Fe I	0.10	177	0.10	178
Fe II	0.10	34	0.10	32
Co I	0.13	19	0.30	21
Ni I	0.07	47	0.10	44
Zn I	0.0	3	0.0	3
Sr I	0.10	1	0.30	3
V I	0.30	6	0.20	3
V II	0.20	3	0.0	2
Zr I	0.40	5	0.50	3
Zr II	0.40	5	0.10	4
Ba II	0.10	5	0.0	5
La II	0.40	4	0.36	5

i) If a close companion heats the facing hemisphere enough to produce the UV excess, at least the U magnitude should vary, unless both binaries are pole on, as the companion revolves round the primary; this variation is not reported. We consider it unlikely that both binaries could be observed pole on, owing to the large distance between ζ^1 and ζ^2 Ret which prevents any efficient dynamical effect to enforce orbits to be coplanar.

ii) Let us consider ζ^1 Ret. We have tried to construct a pair of main sequence stars the combined colours of which fit the observed ones, using the colour index versus $T_{\rm eff}$ calibration of Johnson (1966). A good fit, except for the U magnitude, is obtained with a primary at $\theta_{\rm eff}=0.85$ and a secondary at $\theta_{\rm eff}=1.02$ (K2V). We have not found any combinations providing a good fit over the whole spectral range from U to K. The combined theoretical Hβ profile fits the observed one well. Consequently the Hβ strip in the diamond diagram of Fig. 2a should be shifted by 0.01 in $\theta_{\rm eff}$ to obtain the diagram corrected for the effect of the secondary. In the same way, we have computed the effect on the ionization equilibrium condition and on the fit of the absolute magnitude, without taking into account a possible heating by the companion, in view of point i) above. The corrected diamond diagram (Da Silva, 1986) is shown in Fig. 4: the three criteria of determination of $\theta_{\rm eff}$ and log g clearly disagree. Similar results are obtained for ζ^2 Ret. Therefore assuming that ζ^1 and ζ^2 Ret are two twin systems does neither allow an internally

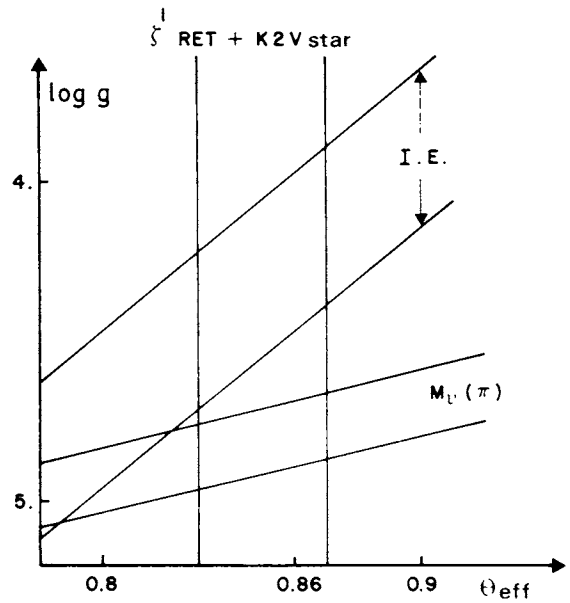

Fig. 4. Same as Fig. 2a but assuming ζ^1 Ret has a close companion of spectral type K2V

consistent determination of the atmospheric parameters from the detailed analysis, nor allow a good match of the observed colours.

iii) Neither ζ^1 nor ζ^2 Ret are known visual binaries. Speckle interferometric observations failed to discover a close companion: the first report of the discovery of a companion for ζ^2 Ret (Bonneau et al., 1980) has been found to be due to an artefact in the diffraction pattern of the telescope spider (Bonneau and Foy, 1986). Therefore neither ζ^1 nor ζ^2 Ret is an interferometric binary, except if the magnitude difference between the components is larger than 3 or the separation is smaller than 0″.02; in the first case, we do not expect a large effect on the U magnitude.

iv) Neither ζ^1 nor ζ^2 Ret are known to have a variable velocity. This is in conflict with the hypothesis that they would have very close companions.

4.3. *An overabundance of helium*

We shall now discuss the hypothesis that the apparent, and abnormal, gravity of ζ^1 and ζ^2 Ret is due to an overabundance of helium in the atmospheres of these stars. The results of Sect. 3 were derived under the assumption that $n({\rm He})/n({\rm H})=0.1$. Let us now assume that $n({\rm He})/n({\rm H})=y$ is larger than 0.1. This hypothesis is in fact strongly supported by the location of ζ^1 and ζ^2 Ret below the main sequence (Johnson et al., 1968), their metal content being solar.

The Hβ profile is insensitive to a change in y at given $T_{\rm eff}$, as discussed by Böhm-Vitense (1979), so that our determination of $\theta_{\rm eff}$ is unaffected. In atmospheres where the metals supply all the electrons and H^- is the source of opacity, helium acts only through its weight. More helium then means less neutral hydrogen per gram or less opacity, and two models with identical $\theta_{\rm eff}$ and $[{\rm M/H}]_\odot^{\rm model}$ but differently will have the same temperature and electron pressure versus optical depth relationship if their gravities g and helium abundances y obey the relation:

$$g'/g''=[(1+y')/(4+4y')]\times[(1+4y'')/(1+y'')] \quad (3)$$

© European Southern Observatory • Provided by the NASA Astrophysics Data System

1987A&A...177..204D

(Strömgren et al., 1982). Then, the spectra corresponding to these two models should be almost identical. It means that we can derive the Helium abundance in ζ^1 and ζ^2 Ret provided we know the actual surface gravity of these stars; with $y > 0.1$, this gravity is smaller than that found in Sect. 3.

In the following calculations, we will assume that the gravity of ζ^1 and ζ^2 Ret should fit that of the ZAMS for the same y, i.e.: that they are not evolved. This could seem to conflict with their kinematical parameters typical of the old disc population. But two arguments support the idea that they are still very near their ZAMS: i) Ca II H and K emission lines are visible in the spectrum of ζ^1 Ret (Foy, 1972a), which means it should be a young star, in the sense it has not evolved markedly from the ZAMS (Wilson and Woolley, 1970), and ii) an effect of the helium overabundance is to slow the stellar evolution across the main sequence at fixed $T_{\rm eff}$ and $[{\rm M/H}]^*_\odot$ due to the lower mass.

Then, since we assume that ζ^1 and ζ^2 Ret are on the ZAMS, Eq. (3) becomes:

$$\log g(\zeta\,{\rm Ret}, y) = \log g\ ({\rm ZAMS}, y) \qquad (4)$$
$$= \log g\ (\zeta\,{\rm Ret},\ 0.1) - \log(1+4y)/(1+y) + 0.105\,,$$

where $g({\rm ZAMS}, y)$ denotes the gravity on the ZAMS for the helium abundance y, with given $T_{\rm eff}$ and $[{\rm M/H}]^*_\odot$. The difference in the determination of the gravities of ζ^1 and ζ^2 Ret is not significant; we will assume $\log g = 4.72$ for both. Then we have:

$$\log g(\zeta\,{\rm Ret}, y) = 4.83 - \log\ (1+4y)/(1+y)\,. \qquad (5)$$

Another, independent, relationship exists between g and y. Indeed an increased helium abundance at constant $[{\rm M/H}]^*_\odot$ implies that Z, the heavy element mass per unit mass, decreases according to:

$$Z = 0.02 \times 1.4/(1+4y) \qquad (6)$$

as derived from Böhm-Vitense (1979); here we assume $Z = 0.02$ and $y = 0.1$ in the solar photosphere. Both the increase in y and the decrease in Z increase the gravity on the ZAMS at given $T_{\rm eff}$, according to:

$$\Delta \log g = \Delta\,[Z]\ \partial \log g/\partial\,[Z] + \Delta y\ \partial \log g/\partial y \qquad (7)$$

with $\Delta\,[Z] = \log(1.4/(1+4y))$. From Hejlesen (1980), we have:

$$\partial \log g/\partial y = 0.82\,{\rm dex} \qquad (8)$$

and

$$\partial \log g/\partial\,[Z] = -0.32\,{\rm dex} \qquad (9)$$

from which it follows from Eq. (6) that the second relationship between the gravity and the helium abundance is:

$$\log g\ ({\rm ZAMS}, y)$$
$$= \log g\ (\zeta\,{\rm Ret}, y)$$
$$= \log g\ ({\rm ZAMS}, 0.1) + 0.82y + 0.32\ \log(1+4y) - 0.129\,. \qquad (10)$$

Solving the system of Eqs. (5) and (10), we find both the helium content in ζ^1 and ζ^2 Ret, and their actual gravity. We have $y = 0.22 \pm 0.04$. The error bar accounts for the error in the adopted gravity only, $\delta = 0.07$, since the error in the determination of $\log g$ for each of ζ^1 and ζ^2 Ret is taken as ± 0.1 dex from Fig. 2.

The resulting actual gravity is:

$$\log g\ (\zeta^1\,{\rm Ret}, 0.22) = \log g\,(\zeta^2\,{\rm Ret}, 0.22) = 4.64 \pm 0.1 \qquad (11)$$

Therefore the ionization equilibrium strips in Fig. 2a and b are to be shifted by $4.64 - 4.72 = -0.08$ dex. Changing the helium abundance also changes the gravity deduced from the trigonometric parallax, since the stellar mass $\mathfrak{M}(y)$ changes in the same amount as $\log g$ (ZAMS), the luminosity being kept constant:

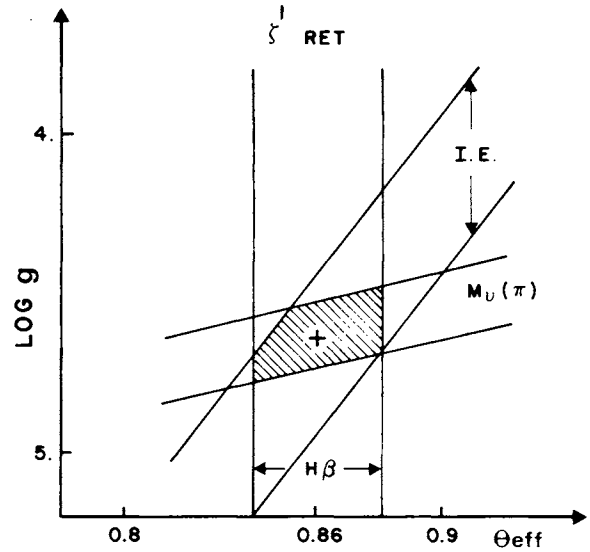

Fig. 5. Same as Fig. 2a but assuming ζ^1 Ret is helium-rich: $n({\rm He})/n({\rm H}) = 0.22$

$$\log \mathfrak{M}(y) - \log \mathfrak{M}(0.1) = -0.14\,. \qquad (12)$$

The absolute magnitude strip in the diamond diagram (Fig. 2) has to be shifted upward by the same amount; it leads to $\log g\ (\zeta^1\,{\rm Ret}) = 4.64$ and $\log g\ (\zeta^2\,{\rm Ret}) = 4.59$ for $\theta_{\rm eff} = 0.83$ and $\theta_{\rm eff} = 0.86$ respectively, which is consistent (Fig. 5) with the above determination.

Thus the final result is:

$$\zeta^1\,{\rm Ret}: \quad \theta_{\rm eff} = 0.86 \pm 0.02;\ \log g = 4.6 \pm 0.1;$$
$$[{\rm Fe/H}]^{\zeta^1}_\odot = +0.1 \pm 0.2;\ n({\rm He})/n({\rm H}) = 0.22 \pm 0.04 \qquad (13)$$

$$\zeta^2\,{\rm Ret}: \quad \theta_{\rm eff} = 0.83 \pm 0.02;\ \log g = 4.6 \pm 0.1;$$
$$[{\rm Fe/H}]^{\zeta^2}_\odot = +0.1 \pm 0.2;\ n({\rm He})/n({\rm H}) = 0.22 \pm 0.04 \qquad (14)$$

We get consistent results assuming that He is overabundant in the atmosphere of ζ^1 and ζ^2 Ret. This overabundance accounts for the high gravity of these G dwarfs having a solar metal content; but it does not explain the discrepancies between the photometric temperatures of Table 1 nor the weakness of the CN band found by Hardorp (1982), at least not for ζ^1 (unless the unknown UV absorber is related to the helium abundance).

It is interesting to note that ζ^1 and ζ^2 Ret would not stand alone. Table 4 lists other possible members of the moving group ζ Her (Woolley, 1970), with their spectral types, trigonometric parallaxes, $B-V$, together with the corresponding absolute magnitude M_v(sp) (Allen, 1973), $M_v(\pi)$, M(ph) and with the UV excess $\delta\,(U-B)$ determined with $B-V$ and the $U-B$ versus $B-V$ calibration by Johnson (1966). Most stars have an UV excess, though not as large as ζ^1 and ζ^2 Ret, except possibly for 1 Hya. Also there are stars having $M_v(\pi)$ larger than M_v(sp) or M_v(ph), which means that they lie below the standard main sequence. None of these stars are known to be metal-poor: again an overabundance of He can account for their low luminosity. If the group ζ Her has a physical existence, would it then be helium rich? Further investigations of stars in this moving group

© European Southern Observatory • Provided by the NASA Astrophysics Data System

1987A&A...177..204D

Table 4. Members of the moving group ζ Her; M_v(sp), $M_v(\pi)$ and M_v(ph) are the absolute magnitudes derived from the spectral type ST from the trigonometric parallax π and from the $B-V$ colour index. $\delta(U-B)$ is the $U-B$ excess relative to $B-V$

Number Gliese	Name	V	$B-V$	$U-B$	SP	π	M_v(sp)	M_v(ph)	$M_v(\pi)$	$\delta(U-B)$
19	β Hyi	2.80	0.06	0.11	G2IV	0″.159	3.0	3.0	3.8	0.04
136	ζ^1 Ret	5.54	0.64	0.08	G2V	0.094	4.7	4.7	5.3	0.10
138	ζ^2 Ret	5.23	0.60	0.01	G1V	0.094	4.5	4.5	5.0	0.11
306	1 Hya	5.60	0.46	−0.06	dF2	0.054	2.9	3.7	4.3	0.06
456		11.30	1.38	1.20	dM1	0.064	9.5	8.6	10.3	0.05
635a	ζ Her	2.81	0.65	0.21	G0IV	0.104	3.1	4.8	2.4	0.0
635b	–	5.49	0.75	0.34	K0V	0.104	5.9	5.5	5.6	0.05
678	–	5.30	0.72	0.30	G8IV-V	0.052	3.2–5.7	3.1–5.2	3.9	0.0
9079	HD 14680	8.81	0.93	–	K3V	0.042	6.6	6.4	6.9	–
9701	ϕ_2 Pav	5.11	0.53	0.01	F8V	0.047	4.0	4.1	3.5	0.04

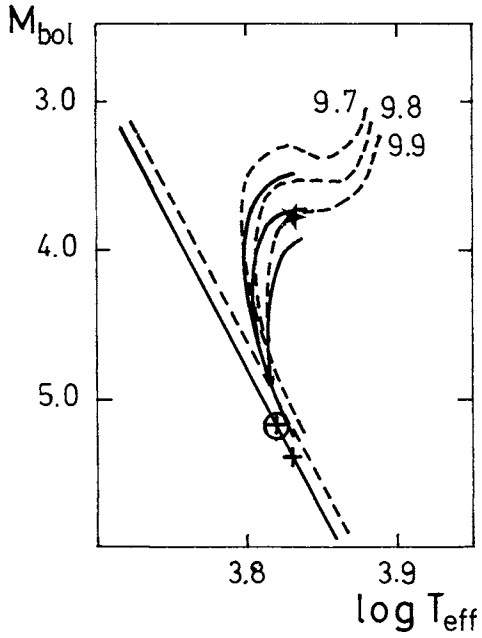

Fig. 6. Location of ζ^1(+) and ζ^2(⊕) Ret and of β Hyi (asterisk) on the theoretical evolutionary tracks ($X=0.6$, $Z=0.02$, $1/\mathrm{Hp}=2.0$) by Hejlesen (1980) (dashed lines), and on the same tracks corrected for the helium overabundance found for ζ^1 and ζ^2 Ret (solid lines)

would be interesting. Proust and Foy (1986) have analyzed in detail β Hyi, another member of the group; they have derived $[\mathrm{Fe/H}]_{\odot}^{\beta\,\mathrm{Hyi}}=0.0\pm0.2$. From the point of view of the heavy element content, β Hyi, ζ^1 and ζ^2 Ret could have a common origin. The absolute magnitude of β Hyi as derived from the trigonometric parallax ($\pi=0''.159$) $M_v=3.8$ is consistent with the spectroscopic gravity $\log g=4.0$. Unfortunately we cannot assign a precise value of $\log g$ from its stage of evolution as we were able to do in the case of ζ^1 and ζ^2 Ret. Therefore it is not possible to discuss the helium abundance of β Hyi. Nevertheless, it should be emphasized that from the point of view of the stellar evolution theory, it could have a common origin with ζ^1 and ζ^2 Ret. Indeed, from the theoretical isochrones of Hejlesen (1980), the effect of a change in the fractional mass of helium y from 0.2, the standard value, to 0.4 (i.e.: $y=0.17$), is to shift the part of the isochrones near the mean sequence downwards by 0.55 magnitude. We would need theoretical isochrones computed for $y\simeq0.48$, which, unfortunately, are not available in the literature. Assuming a linear extrapolation is correct at first order, we derive that a change from $y=0.4$ to $y=0.48$ is equivalent to a shift in M_{bol} of 0.2 magnitude. The resulting isochrones near the main sequence for $y=0.52$ are shown in Fig. 6, as well as the location of ζ^1 and ζ^2 Ret and of β Hyi. The three stars could lie on the same isochrone log age = 9.8: they could have a common origin.

Finally, we would point out that the cosmic scatter of the helium abundance even in the solar neighborhood could be much larger than assumed in current models of the chemical evolution of the Galaxy. Strömgren et al. (1982) have given evidence for the idea that the Hyades would be helium-poor, which agrees with a previous analysis of this problem by Cayrel de Strobel (1979). Now we have found a twin system in which the helium abundance seems to be twice as high as in the solar photosphere. Accurate parallaxes as expected from the Hipparcos satellite and high signal to noise ratio spectroscopy would allow an extended study of the helium abundance in unevolved stars in the solar vicinity, in order to provide new input parameters in the astration models and perhaps, as a further consequence, in cosmogonic models also.

Acknowledgements. We thank B. Gustafsson and G. Odgers for a critical reading of the manuscript, and the referee J. Hardorp. One of us (L.D.) is grateful to the CNPQ, Brazil, for a grant (Nr. 402540-84) to go to France which has enabled us to finish this work.

References

Allen C.W.: 1973, Astrophysical Quantities, The Athlone Press, Univ. of London

Blanc-Vaziaga, M.-J., Cayrel, G., Cayrel, R.: 1973, *Astrophys. J.* **180**, 871

Böhm-Vitense, E.: 1979, *Astrophys. J.* **234**, 521

Bonneau, D., Blazit, A., Foy, R., Labeyrie, A.: 1980, *Astron. Astrophys. Suppl.* **42**, 185

Bonneau, D., Foy, R.: 1986 (in preparation)

© European Southern Observatory • Provided by the NASA Astrophysics Data System

1987A&A...177..204D

Cayrel de Strobel, G.: 1979, in *Stars Clusters, IAU Symp.* **85**, ed. J.E. Hesser, Reidel, Dordrecht, p. 91
Danziger, I.J.: 1966, *Astrophys. J.* **143**, 527
Da Silva, L.: 1975, *Astron. Astrophys.* **41**, 287
Da Silva, L.: 1986, *Astron. J.* (submitted)
Eggen, O.J.: 1958, *Monthly Notices Roy. Astron. Soc.* **118**, 154
Foy, R.: 1971, *Astron. Astrophys.* **11**, 89
Foy, R.: 1972a, in *L'âge des étoiles, IAU Coll.* **17**, eds. G. Cayrel de Strobel, A.-M. Delplace, Paris-Meudon Observatory, p. XLVI-1
Foy, R.: 1972b, *Astron. Astrophys.* **18**, 26
Gehren, T.: 1981, *Astron. Astrophys.* **100**, 97
Hardorp, J.: 1982, *Astron. Astrophys.* **105**, 120
Hearnshaw, J.B.: 1975, *Astron. Astrophys.* **38**, 271
Hejlesen, P.M.: 1980, *Astron. Astrophys. Suppl.* **39**, 347
Hoffleit, D., Jaschek, C.: 1982, *The Bright Stars Catalogue*, Yale Univ. Observatory
Johnson, H.L.: 1966, *Ann. Rev. Astron. Astrophys.* **4**, 193
Johnson, H.L., MacArthur, J.W., Mitchell, R.I.: 1968, *Astrophys. J.* **152**, 465
Keenan, D.W., Yorka: 1985, *Stand. Star Newsl.* **6**, 1985
Koornneef, J.: 1983, *Astron. Astrophys. Suppl.* **51**, 489
Kovacs, N., Foy, R.: 1977, *Astron. Astrophys.* **57**, 235
Labs, D., Neckel, H.: 1968, *Zf. A* **69**, 1
Moore, C.E., Minnaert, M.J.G., Houtgast, J.: 1966, *Nat. Bur. Stand. Monog.* **61**
Peytremann, E.: 1974a, *Astron. Astrophys.* **33**, 203
Peytremann, E.: 1974b, *Astron. Astrophys. Suppl.* **18**, 81
Praderie, F.: 1967, *Ann. Astrophys.* **30**, 31
Proust, D., Foy, R.: 1986, *Astron. Astrophys.* (submitted)
Strömgren, B., Olsen, E.H., Gustafsson, B.: 1982, *Publ. Astron. Soc. Pacific* **94**, 5
Wilson, O.C., Woolley, R.: 1970, *Monthly Notices Roy. Astron. Soc.* **148**, 463
Woolley, R.: 1970, in *Galactic Astronomy*, eds. H.Y. Chiu, A. Muriel, Gordon and Breach, New York, p. 95

© European Southern Observatory • Provided by the NASA Astrophysics Data System